



LAWRENCE
LIVERMORE
NATIONAL
LABORATORY

Density Distributions in TATB Prepared by Various Methods

D. M. Hoffman, A. T. Fontes

May 15, 2008

Propellants, Explosives, Pyrotechnics

Disclaimer

This document was prepared as an account of work sponsored by an agency of the United States government. Neither the United States government nor Lawrence Livermore National Security, LLC, nor any of their employees makes any warranty, expressed or implied, or assumes any legal liability or responsibility for the accuracy, completeness, or usefulness of any information, apparatus, product, or process disclosed, or represents that its use would not infringe privately owned rights. Reference herein to any specific commercial product, process, or service by trade name, trademark, manufacturer, or otherwise does not necessarily constitute or imply its endorsement, recommendation, or favoring by the United States government or Lawrence Livermore National Security, LLC. The views and opinions of authors expressed herein do not necessarily state or reflect those of the United States government or Lawrence Livermore National Security, LLC, and shall not be used for advertising or product endorsement purposes.

Density Distributions in TATB Prepared by Various Methods

D. Mark Hoffman and Aaron T. Fontes
Lawrence Livermore National Laboratory
Livermore, CA 94550

ABSTRACT:

The density distribution of two legacy types of 1,3,5-triamino-2,4,6-trinitrobenzene (TATB) particles were compared with TATB synthesized by new routes and recrystallized in several different solvents using a density gradient technique. Legacy wet (WA) and dry aminated (DA) TATB crystalline aggregates gave average densities of 1.9157 and 1.9163 g/cc, respectively. Since the theoretical maximum density (TMD) for a perfect crystal is 1.937 g/cc, legacy TATB crystals averaged 99% of TMD or about 1% voids. TATB synthesized from phloroglucinol (P) had comparable particle size to legacy TATBs, but significantly lower density, 1.8340 g/cc. TATB synthesized from 3,5-dibromoanisole (BA) was very difficult to measure because it contained extremely fine particles, but had an average density of 1.8043 g/cc over a very broad range. Density distributions of TATB recrystallized from dimethylsulfoxide (DMSO), sulfolane, and an 80/20 mixture of DMSO with the ionic liquid 1-ethyl-3-methyl-imidazolium acetate (EMImOAc), with some exceptions, gave average densities comparable or better than the legacy TATBs.

INTRODUCTION:

The Department of Energy (DOE) uses TATB as an insensitive high explosive (IHE), but has not purchased this material since the late 1980. With increasing safety concerns, the Department of Defense (DoD) has become interested in TATB and begun evaluating new sources.[1, 2] Lawrence Livermore National Laboratory (LLNL) evaluated two of these new TATBs and found significant differences between them and the legacy TATBs used by DOE in the past. [3] Since no drop-in replacement for legacy TATB was available, LLNL was also interested in improving the crystal quality of new TATB and recovering legacy TATB from its plastic bonded explosives (PBXs) as systems are being retired. To determine if new or recrystallized TATB meets current DOE needs requires several metrics for comparison with what was used previously. Although the density gradient technique is tedious, it seems to be applicable in this area.

The initiation and subsequent transition to sustained detonation of an explosive is believed to be associated with the adiabatic compression of voids or “hot spots” in the explosive. [4, 5] Recently it has been shown that for non-ideal explosives the critical energy or pressure of initiation is a function of the density.[6] This being the case, the quality of explosive crystals is expected to impact their initiability. A variety of methods have been used to assess the crystal quality of different explosives on various length scales[7]. Differential scanning calorimetry (DSC)[8, 9] shows reduction in the melting point of crystals containing impurities or of small size or perhaps with varying degree of defects. Using ultra small angle x-ray scattering (USAXS) [10] the distribution of void volume of pressed pellets and powders has been evaluated over the size range from a few

nanometers to several micrometers. Old standby techniques like optical microscopy (OM) [11-13] and scanning electron microscopy (SEM) [14] have been used for many years, but are limited to about 0.2 μm resolution in the former case and to surface defects in the latter. Frequency broadening of the ^{16}N quadrupole (NQR) in spin-lattice relaxations of the crystal has been used to differentiate insensitive RDX[9, 15, 16] and CL-20 crystals and plastic bonded explosive (PBX) formulations [17, 18]. Any interruption of the crystal lattice of an explosive will also affect the crystal density [12, 19-21]. Density was chosen for this effort because of its simplicity and our familiarity with the technique. All of these methods and others have limitations and results often fail to identify the root cause of changes in initiability because an explosive formulation is generally not composed of crystalline particles only. Furthermore, assumptions about the nature of the flaws measured by a technique cloud the interpretation of the results.

The standard methods for determining PBX or crystal densities are immersion [ptx proc] and pycnometry [22] which yield an average density of the sample contained in the vessel. Two methods for evaluating the density distribution have been used on explosive and other crystals recently. The flotation method [12, 23, 24] uses different density fluids to float off cuts of crystalline explosive and generates a distribution curve from these. The density distribution measured in this article used the gradient method. [25, 26] This method has been used to distinguish different types of RDX [19] and density differences associated with crystallization techniques used with ϵ -CL-20. [20].

Crystal quality depends on crystal growth rate which, in turn, depends on the dissolution temperature, the energetics of the growth face with the mother liquor and degree of super saturation. Typically commercial crystallization processes are designed around cost effectiveness rather than optimum crystal quality.

EXPERIMENTAL:

Materials: WA TATB (C-084; 13-03-85-0307-538) and DA TATB (C-090; 12-03-82-0324-273) were synthesized by Aerojet Corporation in 1985 and 1982, respectively. A dry aminated TATB synthesized in 1977 (B 484; 1B-034-108) by Cordova was also tested. TATB synthesized from Phloroglucinol (C-562 TATB001) and from 3,5 dibromoanisole (C-559 BAE6E295-001) were graciously provided by the Naval Surface Warfare Center at China Lake, CA. Recrystallization solvents were used as received. TATB recrystallized from DMSO has been described previously. [27, 28] Recrystallization of TATB from the ionic liquid 1-ethyl-3-methyl imidazolium acetate (EMImOAc) in DMSO:20/80 by weight [29] and from sulfolane [3] are described elsewhere.

Density gradient technique: The density gradient technique has been described previously.[20] Several thousand crystals of TATB were counted for most samples in the gradient column. Two ZnBr_2 /water solutions of approximately 1.84 and 2.00 g/cc were used to prepare each column. Except for BA TATB, 7 calibration beads with densities of 1.96, 1.94, 1.92, 1.91, 1.8705, 1.86, and 1.8399, obtained from American Density Co., were used to calibrate the column. Slight curvature in calibration for some TATBs gave

resulted in which about 0.01% of the crystals appear to have density greater than TMD. Linear calibration of column height against calibration beads for WA TATB gave correlation coefficient of 0.9999. The number average density $\langle \rho \rangle$ is calculated by:

$$\langle \rho \rangle = \sum_i n_i \rho_i / \sum_i n_i = N^{-1} \sum_i n_i \rho_i = \sum_i r_i \rho_i \quad (1)$$

Where n_i , r_i and ρ_i are the number of particles, the relative frequency of particles of density i and N is the total number of particles counted.

Scanning electron microscopy (SEM) was performed using a LEO 438 VP (variable pressure) SEM. The variable pressure SEM reduces surface charging of an organic sample by allowing a low-pressure atmosphere to pass over the sample [30]. This eliminated the need for a conductive surface coating. TATB crystals were sprinkled on an aluminum stud covered with carbon filled tape and examined without further preparation.

RESULTS:

Density Distributions in Legacy TATBs: Legacy TATBs were synthesized from 1,3,5-trichlorobenzene by a dry[31] or a wet [32] amination process. Three manufacturers produced the explosive including Cordova and Aerojet. Density distributions of preproduction (1977) DA TATB made by Cordova and stockpile DA TATB from Aerojet (1982) in Figure 1 show improvement in the density from inception to final product. The average density of the preproduction material was 1.9103 g/cc (98.6% TMD). Possibly over time or due to different crystallization conditions, the production DA TATB (C-090) density improved to about 99% TMD (1.9163 g/cc). In all density distribution plots the %TMD and % voids are given on the upper y-axis based on:

$$\%TMD = 100 * \rho_i / TMD \text{ and } \% \text{ voids} = 100 - \%TMD \quad (2)$$

This assumes that the void density is negligible. It is well known that the dry amination process incorporates approximately 0.5% residual ammonium chloride in the TATB crystal even after washing. The 0.5-2 μm holes seen on the surface of DA TATB crystals in Figure 2a are associated with washing out residual ammonium chloride. If the preproduction TATB was poorly washed and occluded ammonium chloride with no voids there could be up to 5.8% in the TATB. Interestingly the width of the distribution of new TATB is greater (0.048 g/cc) than that for the preproduction TATB (0.027 g/cc).

The wet amination synthesis of TATB (C-084) reduced the residual ammonium chloride to 0.1% or less. The density distribution for the C-084 lot of WA TATB is shown in Figure 3. It compares very well to C-090 DA TATB with average density of 1.9173 g/cc or about 99% TMD. The width of this distribution is intermediate between the two dry aminated TATBs. The SEM of this WA TATB in Figure 2b showed none of the surface voids seen in the DA explosive (Fig 2a).

Density Distriubtions of new TATBs. Because of the limited availability of the chlorinated precursor, commercial manufacturers have scaled up new synthesis routes[1, 2] in support of the DoD Manufacturing Technology (MANTEC) effort. We were interested in new sources of TATB and evaluated two of these TATBs [3]. The density distributions are given in Figure 4. The TATB synthesized from Phloroglucinol (P TATB) had a narrow distribution (0.057 g/cc) about a low average density (1.834 g/cc) or about 94.7% TMD. The TATB based on dibromoaniline (BA TATB) was very fine and difficult to measure. The figure shows a broad distribution over almost 0.2 g/cc about the mean of 1.8043 g/cc or 93.2% TMD. Although most of the particles in BA TATB were very fine (2-3 μ m) and very difficult to count, in the density range of 1.91 g/cc there were a group of large particles (see Figure 5). This shows up as a small jump in the distribution around this value. The data show about 0.14% of these with density greater than TMD.

Table 1. Average crystal density and light scattering particle size (LS PS) of various TATBs evaluated in this work.

Series ID	< ρ > g/cc	% TMD	% voids	LS PS (μ m)
WA	1.9157	98.90	1.10	63 \pm 3
DA-pre	1.9103	98.62	1.38	
DA	1.9163	99.83	1.07	70 \pm 2
P	1.8340	94.68	5.32	56 \pm 0.2
BA	1.8043	93.15	6.85	2.1 \pm 0.2
Sulfolane-P	1.9091	98.56	1.44	140 \pm 32*
Sulfolane-BA	1.9093	98.57	1.43	73 \pm 28*
Sulfolane-L	1.9154	98.88	1.12	130 \pm 60*
DMSO	1.9225	99.25	0.75	420 \pm 90*
B-1	1.8890	97.52	2.48	16.1 \pm 0.3
C-1 IL-50g	1.9276	99.51	0.49	47.9 \pm 1.4
C-2 IL	1.9106	98.64	1.36	126 \pm 13
C-3 IL-50g	1.8833	97.23	2.77	14.6 \pm 0.4
C-4 60°C	1.9215	99.20	0.80	118 \pm 10
D-1 IL-50g	1.9247	99.36	0.64	95.3 \pm 17
E-1 IL – 50g	1.9208	99.16	0.84	47.5 \pm 4
SU-1-1	1.8947	97.81	2.19	159 \pm 82
SU-1-2	1.8617	96.11	3.89	7.53 \pm .04
SU-2-1	1.8912	97.64	2.36	41 \pm 2
SU-2-2	1.8720	96.65	3.36	6.70 \pm .03

* Optical microscope measurements rather than light scattering.

Density Distributions of TATB Recrystallized from Conventional Solvents. A number of studies have been made of solvents for TATB. [27, 28, 33] WA TATB recrystallized in DMSO from reference 23 gave the density distribution shown in Figure 6. The average density was 1.9225 g/cc or about 99.25 % TMD. This recrystallized TATB had very large crystals (some larger than 500 μ m). This 50 g scale crystallization with slow cooling produced large crystals with good density. Due to temperature and time control issues and large quantities of DMSO, smaller scale recrystallization using sulfolane with

rapid dissolution and cooling produced was evaluated. The goal of this effort was improving the average density of new TATBs. There is also interest in possible recovery of stockpile returned LX-17 and PBX 9502 (TATB/Kel-F 800 plastic bonded explosives). Figure 7 shows the density distributions of TATB recrystallized in sulfolane from P TATB, BA TATB and LX-17-1. These recrystallized TATB densities averaged 1.9091, 1.9093, and 1.9154 g/cc, respectively. The percent of TMD averaged 98.6, 98.6 and 98.9%, all within experimental error of the density of the legacy TATBs.

Density Distriubtions of TATB Recrystallized from Ionic Liquids. Because of the low solubility of TATB in conventional solvents, an effort to recrystallize this explosive using ionic liquids (IL) as co-solvents is being investigated. [34, 35] [provisional patent] Table 3 shows several sets of density results from IL/DMSO crystallizations. Typical crystallizations involve heating to 90°C in about 30 minutes, then cooling at different rates to an isothermal temperature. These conditions enable solubilization of upwards of 9-10%. Unfortunately, Meisenheimer complexation of TATB with the IL prevents precipitate and only 60-70% or less is recovered. Samples C-1, E-1, C-4 and C-3 were cooled from 90°C at -0.83 °/h, -1.3 °/h, -1/3 °/min and -0.5 °/min and crystallized at 50, 50, 60 and 70°C, respectively. Sample D-1 was heated to 90°C and allowed to cool to ambient at about -0.1 °/min with no isothermal treatment. Sample C-2 was precipitated after C-1 by addition of water. Figure 8 shows the thermal history of these and the scale up crystallizations.

Figure 9 shows the density distributions of these IL recrystallized TATBs. Sample B, the first attempt to crystallize 50 grams of TATB, was not washed adequately so the density was only 1.889 g/cc. Low levels of residual IL on the TATB crystals can alter their density significantly. Once the washing procedure was developed, the precipitate C-1 slowly cooled from 90 to 50°C produced excellent density (1.9277 g/cc) and morphology. C-3 and C-4 were attempts at isothermal crystallization with rapid cooling rates at 70 and 60°C, respectively. At 70°C the growth rate is relatively slow and small crystals were produced. However, long times at this temperature result in decomposition of the Meisenheimer complex to ADNP reducing the density to 1.883 g/cc. Good density (1.9215 g/cc) and the largest crystals (~100 µm) were obtained from isothermal crystallization at 60°C for approximately 12 h in sample C-4. Sample D1 which was not held at any temperature had a density of 1.9260 g/cc and crystals averaging 90 µm. It may be that most of the crystallization in C-1 and E-1 occurred prior to the isothermal hold. All samples recrystallized below 70°C, except for B-1, had very good density: C1, C4, D1 and E1 had 1.9276, 1.9215, 1.9247, and 1.9208 g/cc, respectively, but only about half of the TATB is recovered in these crystallizations. More TATB could be recovered from the residue liquor using excess water. C-2 is a typical example. The C-2 precipitate had much lower density (1.906 g/cc). The reproducibility of the C-1 process is shown by comparing this density distribution with E-1 which was crystallized following nearly the same procedure.

Two attempts were made to scale up (SU-1 and SU-2) the 20/80:EMIMOAc:DMSO recrystallization to 1 Kg batch size. The thermal history traces in Figure 7 show long times at 90°C compared to the small batches. The scale up produced 2 batches of crystals.

The first precipitate was obtained during cooling. Subsequently the residual TATB was precipitated with water. The presence of 4% water in these mixes led to decomposition of the Meisenheimer complex to ADNP at the elevated temperatures and although large crystals were obtained in the first precipitate, significant reduction in density was observed, as shown in Figure 10. Densities of the first scale up precipitate (SU-1-1) averaged 1.8947 g/cc or 97.8% TMD. As in the case of C1 and C2 above, the second (water) precipitate (SU-1-2) gave lower density, 1.8617 g/cc or 96.1%TMD. Similar results were obtained in the subsequent scale up. The first precipitate (SU-2-1) and second aqueous precipitate had average densities of 1.8912 or 1.872 g/cc, respectively. Results are tabulated in Table 1.

DISCUSSION:

Descriptive statistics for legacy and conventional solvent recrystallized TATB, shown in Table 2, were calculated using the Stat::Fit program [36]. All of the samples had comparable densities and gave negative values for skew compared to the mean (number density according to equation 1). This implies that the distributions are all asymmetric with tails toward lower values of crystal density as can be seen in Figures 1, 3, 6 and 7. The distributions are all leptokurtic, implying more peakedness than a normal distribution. This would seem to imply that the incorporation of voids in the legacy and conventional solvent recrystallization occurs in similar fashion.

Table 2. Descriptive statistics for various distributions of legacy and precipitated TATBs were similar.

Sample ID	C-084	C-090	sATK	sBAE	sLX17	DMSO
No. pts.	7803	7425	6234	7750	6453	412
minimum	1.8903	1.89039	1.85032	1.84892	1.85764	1.89032
maximum	1.9294	1.93844	1.94154	1.94143	1.94112	1.9349
mean	1.91569	1.91634	1.90901	1.90931	1.91538	1.92255
median	1.9173	1.9181	1.91323	1.91314	1.91934	1.9259
mode	1.9184	1.9217	1.91834	1.91199	1.91825	1.92705
std dev	6.39E-03	8.32E-03	1.66E-02	1.50E-02	1.34E-02	1.02E-02
variance	4.08E-05	6.92E-05	2.74E-04	2.26E-04	1.79E-04	1.04E-04
Coef of var	0.333433	0.434133	0.867586	0.78788	0.697884	0.53033
skewness	-1.08362	-0.79033	-0.86701	-1.03952	-1.34771	-1.34849
kurtosis	1.28044	0.34169	0.114266	0.854536	1.74693	1.25278

Densities of TATB recrystallized from IL/DMSO showed two types of distributions depending on the thermal history of crystallization. Crystallization from IL cosolvent systems that occurred under non-isothermal conditions tended to have broad density distribution (D-1). Since C-1, C-3 and E-1 all have broad distributions (C-1 and C-3 have negative kurtosis), it would seem that most of the crystals formed during cooling rather than under isothermal conditions. This seems to indicate that crystals grew over a

broad degree of supercooling and concentrations. On the other hand, C-4 was cooled to 60°C and isothermally crystallized for 2 h. Here the density distribution is sharp (leptokurtic). In this case most of the crystals grew isothermally at a constant supercooling with only concentration affecting the kinetics. Therefore the distribution shows a narrow peak (kurtosis of 2 – highest of all distributions). The negative skew is associated the low density tail from crystals of poor quality formed during the final cool down.

All samples, except B-1 were washed in hot methanol to remove residual mother liquor. Table 3. Thermal history of small scale IL/DMSO recrystallizations of TATB.

Sample ID	B-1	C-1	C-3	C-4	D-1	E-1
td	30 min	30 min	30 min	30 min	30 min	30 min
Td	90C	90C	90	90	90	90
t ramp1, 2	3 h, 3 h	48 h	1 h	1 h	na	30 h
Ti	70, 50C	50C	70C	60 C	na	50C
ti	3h	24 h	15 h	12 h	na	24 h
Cool t		20 h		na	24 h	24 h
T cool	RT	RT	RT	na	RT	
precipitate		no				
Hot wash		MeOH	MeOH	MeOH	MeOH	MeOH

* C-2 was precipitated with water from residual liquor from C-1. Where no value is listed sample was allowed to cool by turning off heat.

The sample crash precipitated with water (C-2) had significantly lower densities but a very leptokurtic distribution. This sharp distribution about a given density appears to be associated with rapid crystallization where changes in solubility occur rapidly due to addition of water or under isothermal conditions, as in C-4. Similar behavior is seen in the second set of precipitations in both scale-up where the residue from the first crystallization was precipitated with excess water (see Fig 10).

Table 3. Descriptive statistics for various distributions of IL recrystallized TATBs were not similar.

Sample ID	C-1	C-2	C-3	C-4	D-1	E-1
No. pts.	2039	1339	7798	1843	3640	4356
minimum	1.91466	1.90065	1.86419	1.90366	1.9078	1.8962
maximum	1.93942	1.91573	1.90762	1.93048	1.9408	1.9363
mean	1.9276	1.9106	1.8833	1.92153	1.92467	1.92081
median	1.9277	1.9107	1.8832	1.9226	1.926	1.92258
mode	1.9228	1.9093	1.88116	1.9226	1.9273	1.918
std dev	5.63E-03	1.87E-03	8.87E-03	4.38E-03	5.92E-03	6.61E-03
variance	3.17E-05	3.49E-06	7.86E-05	1.92E-05	3.50E-05	4.37E-05
Coef of var	0.292134	9.78E-02	0.470892	0.227838	0.307431	0.343977
skewness	1.14E-02	-1.35915	0.115844	-1.491	-0.4814	-0.85296
kurtosis	-0.92276	3.29699	-0.73368	2.07275	0.139658	0.922912

Table 4. Descriptive statistics for 1 Kg scale up TATB recrystallization from IL/DMSO.

Sample ID	Su1-1	Su1-2	Su2-1	Su2-2
No. pts.	4954	20227	19343	4115
minimum	1.8667	1.8457	1.8642	1.8626
maximum	1.9401	1.9364	1.9403	1.8812
mean	1.8947	1.8617	1.8912	1.8720
median	1.9028	1.891	1.9023	1.8719
mode	1.983	1.8588	1.8876	1.8719
std dev	1.12E-2	1.28E-2	1.33E-2	2.76E-3
variance	1.24E-4	1.64E-4	1.77E-4	7.61E-6
skewness	1.54	3.69	0.661	0.540
kurtosis	3.911	*	0.111	0.7522

* large cloud of small particles near the mean could not be counted with any accuracy so the peakedness of the distribution could not be measured accurately.

CONCLUSIONS:

The density gradient method is easily adapted to evaluation of the density distribution of various methods of preparation of TATB crystals. It gives clear comparisons of the density of most of the TATBs tested. The presence of small micrometer sized holes in the dry aminated TATB did not seem to interfere with the measurement. The TATB recrystallized from conventional solvent all had similar shaped distributions with good densities. The TATB synthesized from phloroglucinol and dibromo anisole had low density. This could be corrected by recrystallization from sulfolane. The TATB recrystallized from IL/DMSO had good density so long as the thermal history did not have prolonged hold times above 60°C. Scale up efforts apparently were held too long at 90°C to allow dissolution of the TATB.

ACKNOWLEDGEMENTS:

We would like to thank Tim Mahoney at China Lake for supplying the new TATB samples. George Overturf, John C. Estill, and Bill Mclean provided funding for this work in conjunction with engineering efforts or Peter Raboin and Angela Cook. Pat Lewis ran the light scattering measurements for particle size distributions. Phil Pagoria, Alex Gash and Yong Han prepared and provided samples of the IL/DMSO recrystallized TATBs. Alex Mitchell provided samples of sulfolane and DMSO recrystallized TATBs. This work performed under the auspices of the U.S. Department of Energy by Lawrence Livermore National Laboratory under Contract DE-AC52-07NA27344.

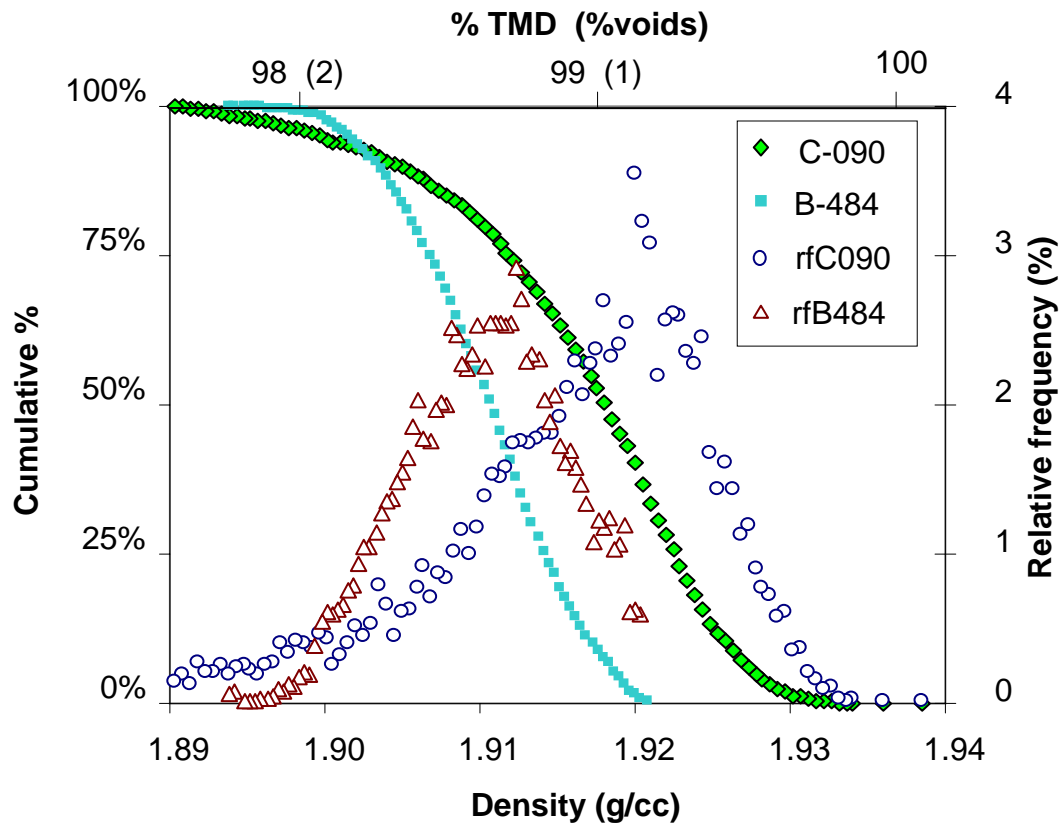


Figure 1. The density distribution of dry aminated TATB made by Aerojet (C090) averaged higher than that made by Cordoba probably because of differences in processing conditions and equipment.

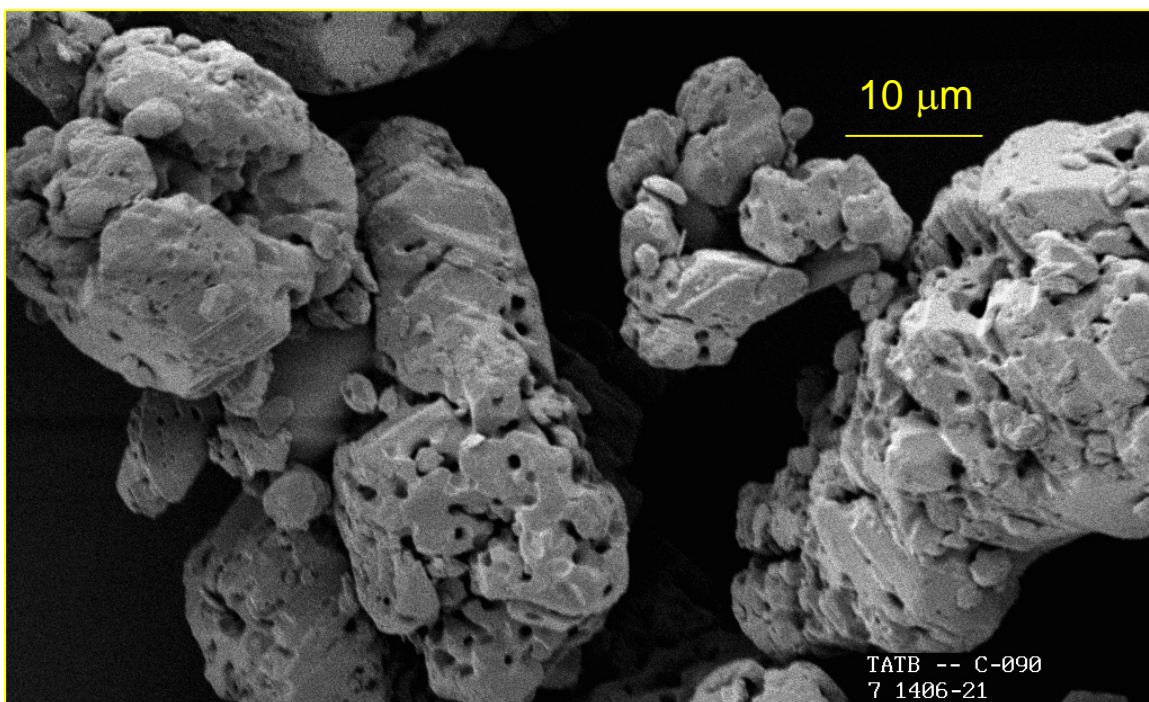
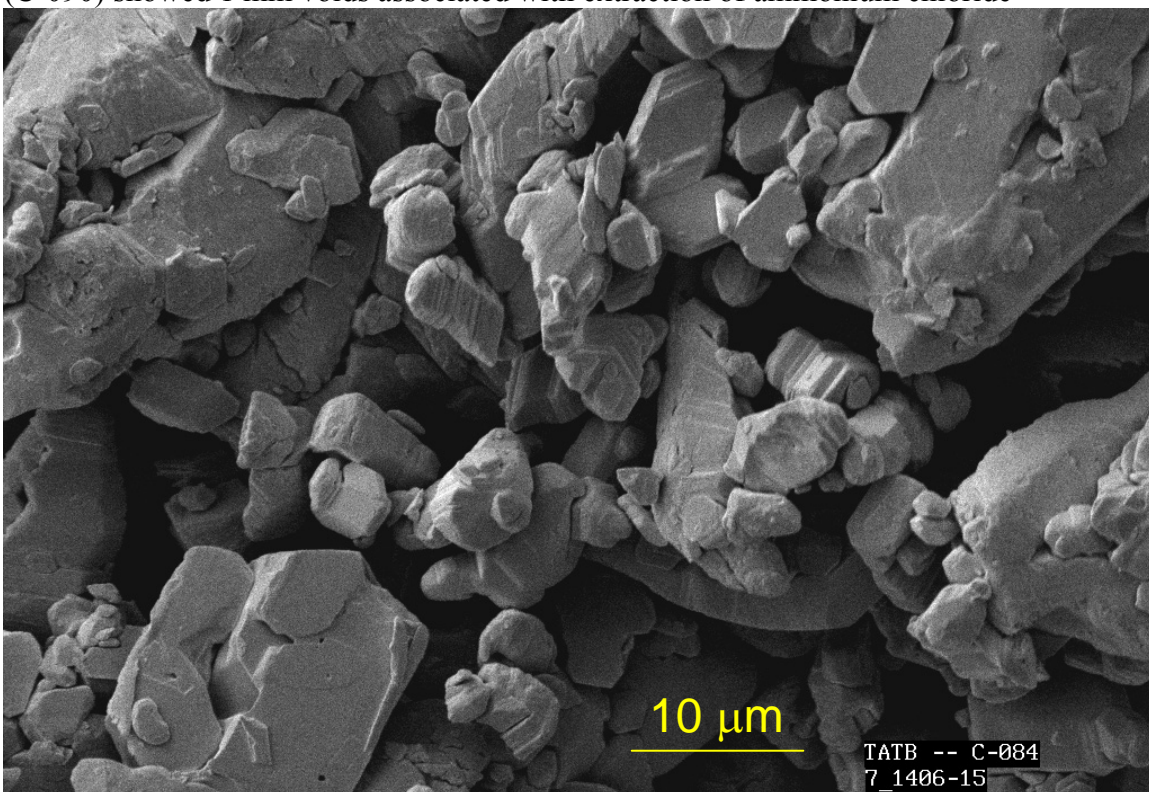


Figure 2a. Scanning electron micrographs of (a) production grade dry aminated TATB (C-090) showed 1 mm voids associated with extraction of ammonium chloride



(2b) The wet aminated TATB (C-084) synthesis produced crystals with substantially reduction of ammonium chloride.

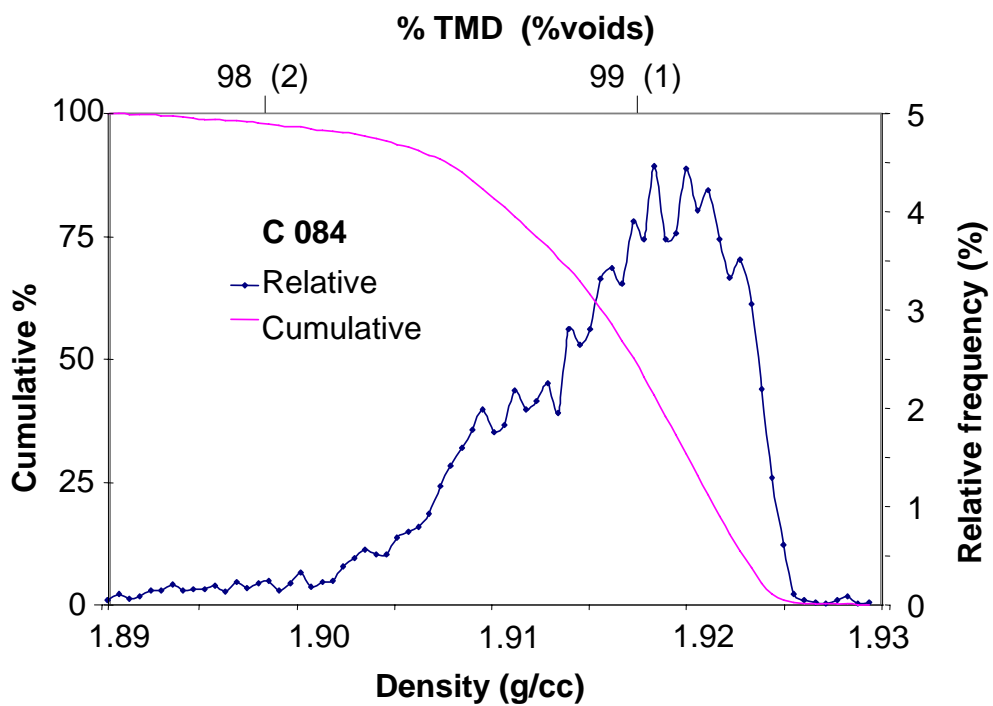


Figure 3. Crystal density distribution of wet aminated TATB averaged about 99% of theoretical maximum.

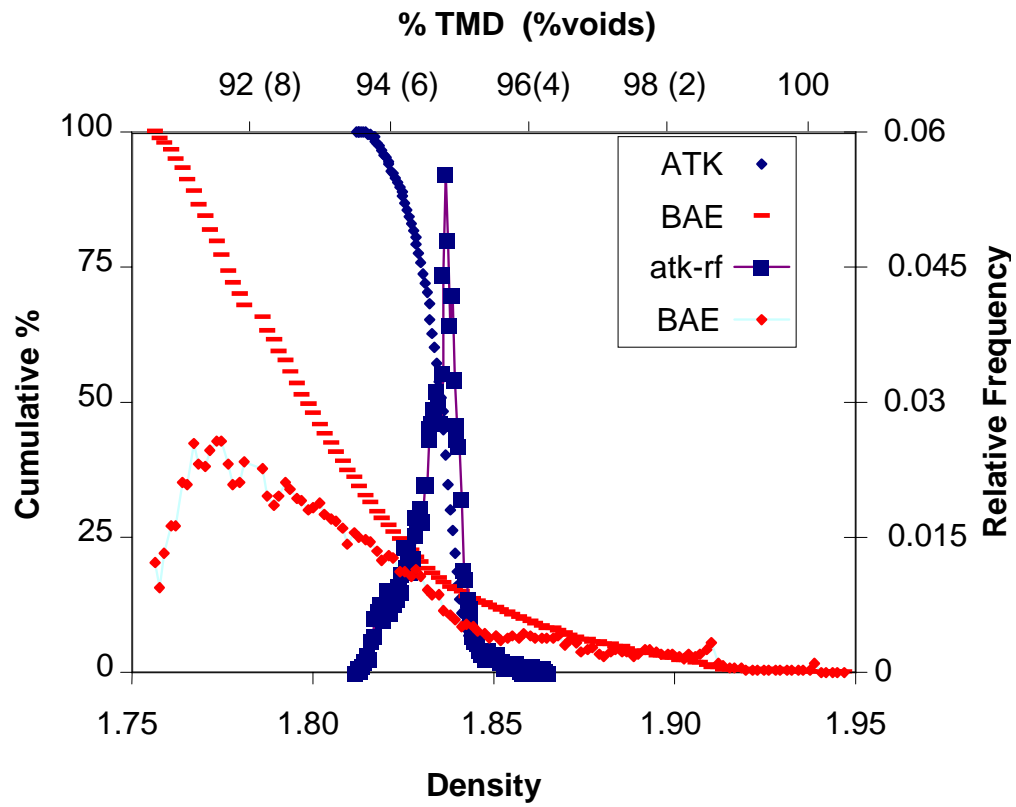


Figure 4. Density distributions of P TATB (narrow) and BA TATB (broad) gave significantly lower average densities based on Eqn. 1 than legacy TATBs.

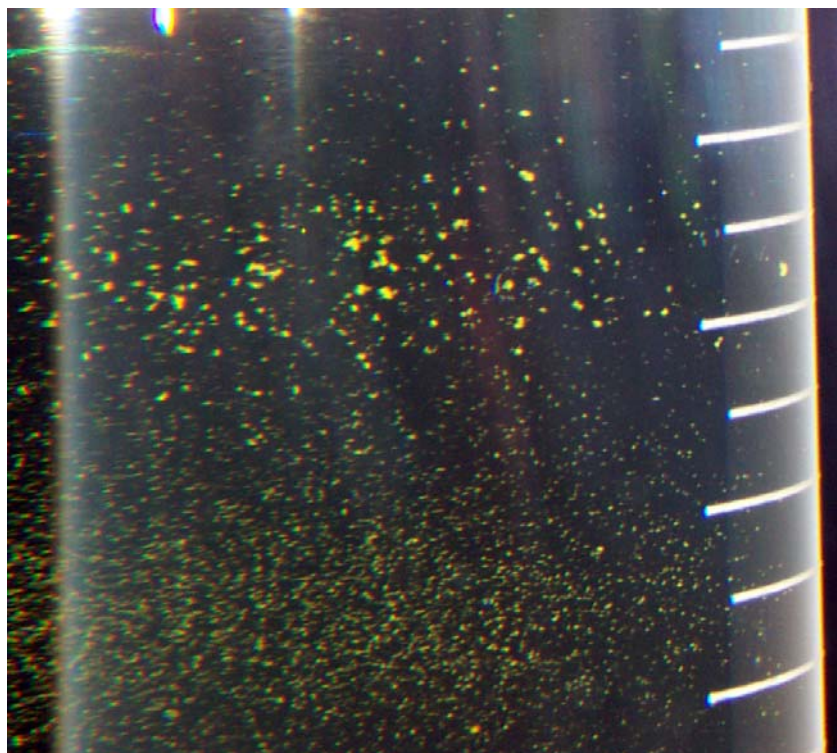


Figure 5. This section of the gradient column of BA TATB shows different sizes of TATB at different densities (density increasing downward).

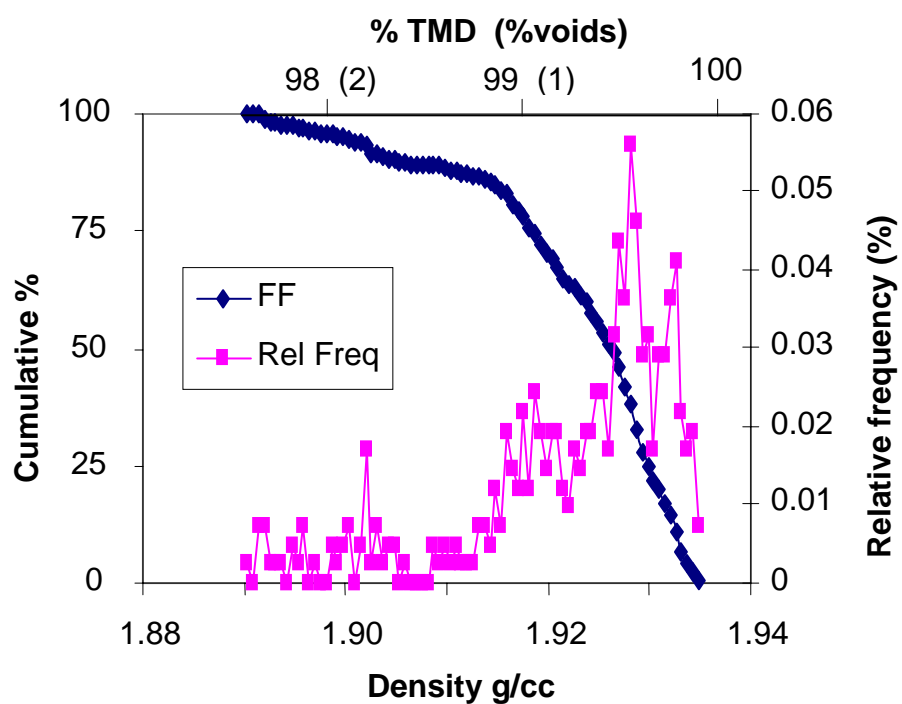


Figure 6. Large TATB crystals produced as part of extensive investigation of recrystallized from DMSO had this density distribution curve.

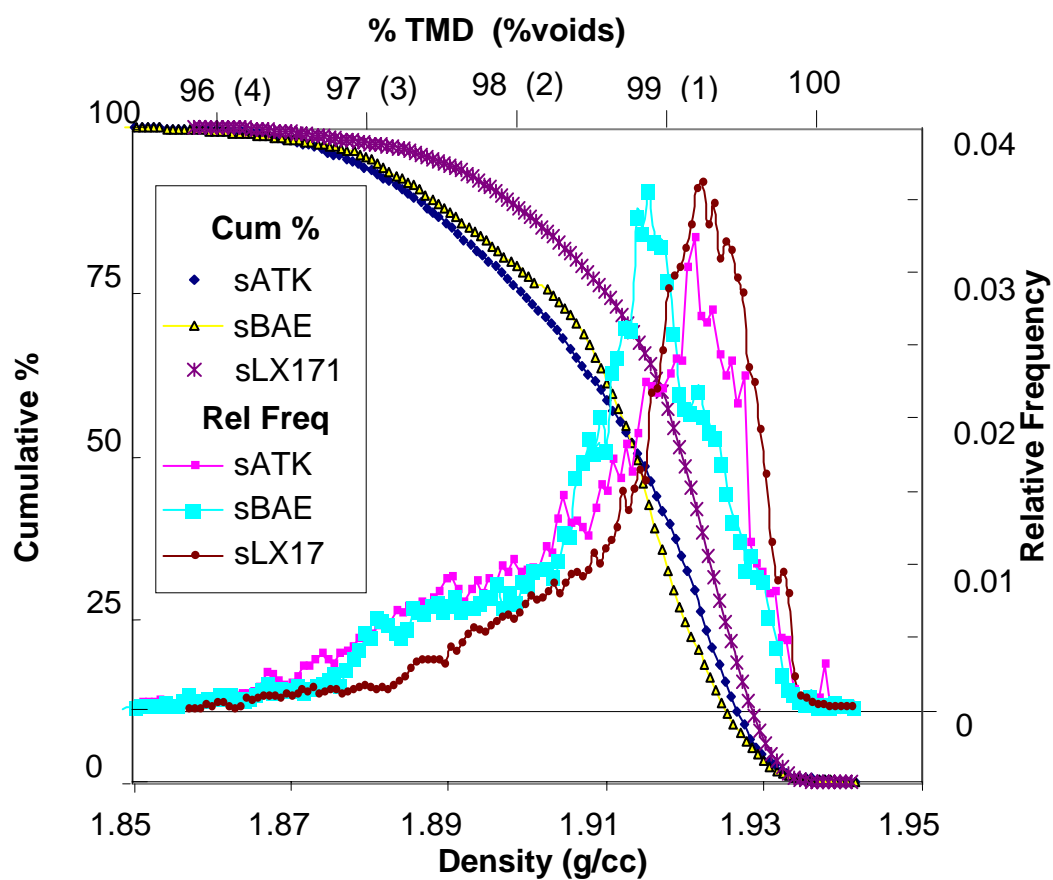


Figure 7. Density distributions of new TATBs recrystallized in sulfolane showed marked improvement.

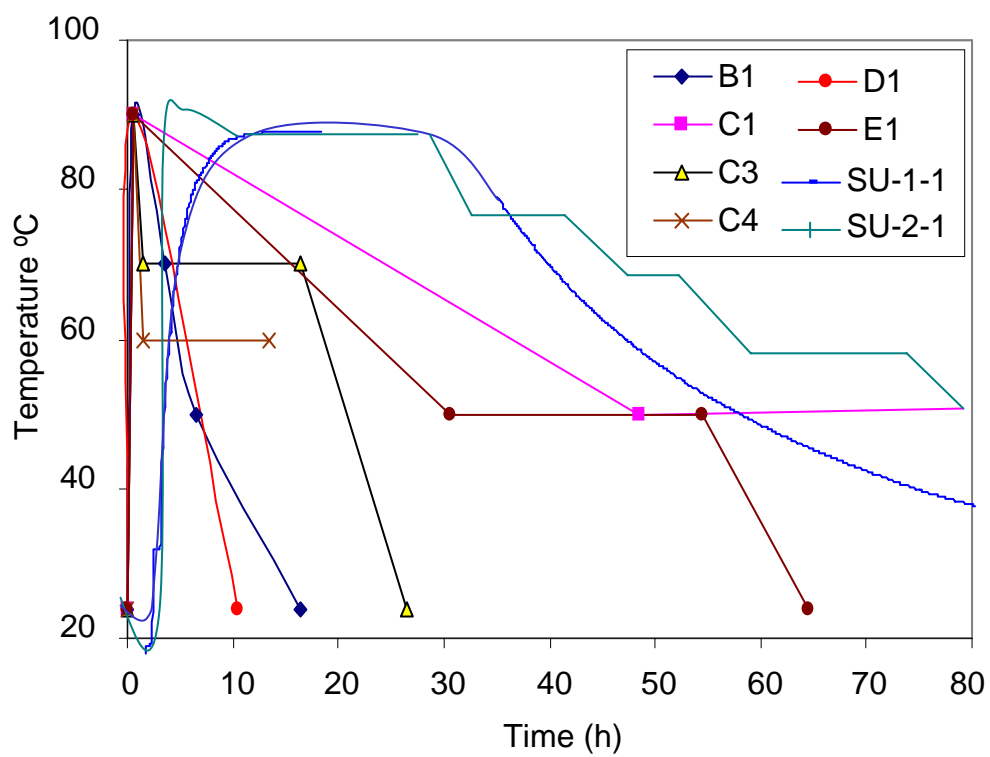


Figure 8. Thermal history of various EMIMOAc/DMSO recrystallizations

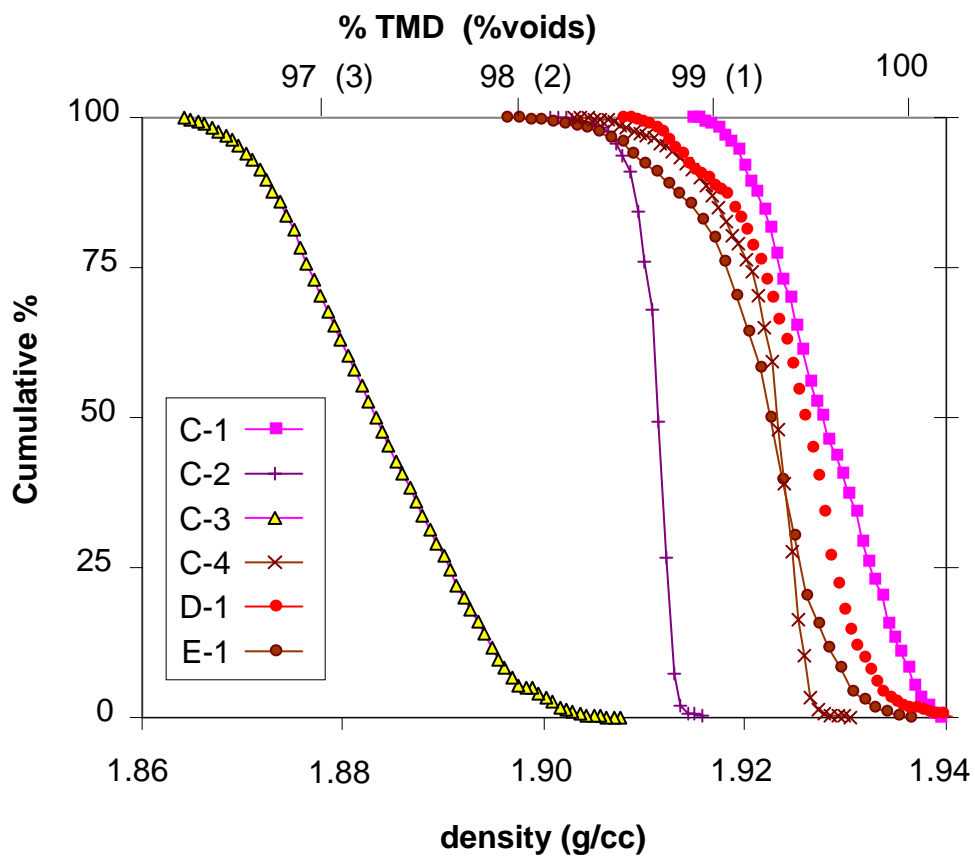


Figure 9. Cumulative density distributions of IL recrystallized TATB indicate that with care superior crystal density compared to the best legacy TATB is attainable via recrystallization.

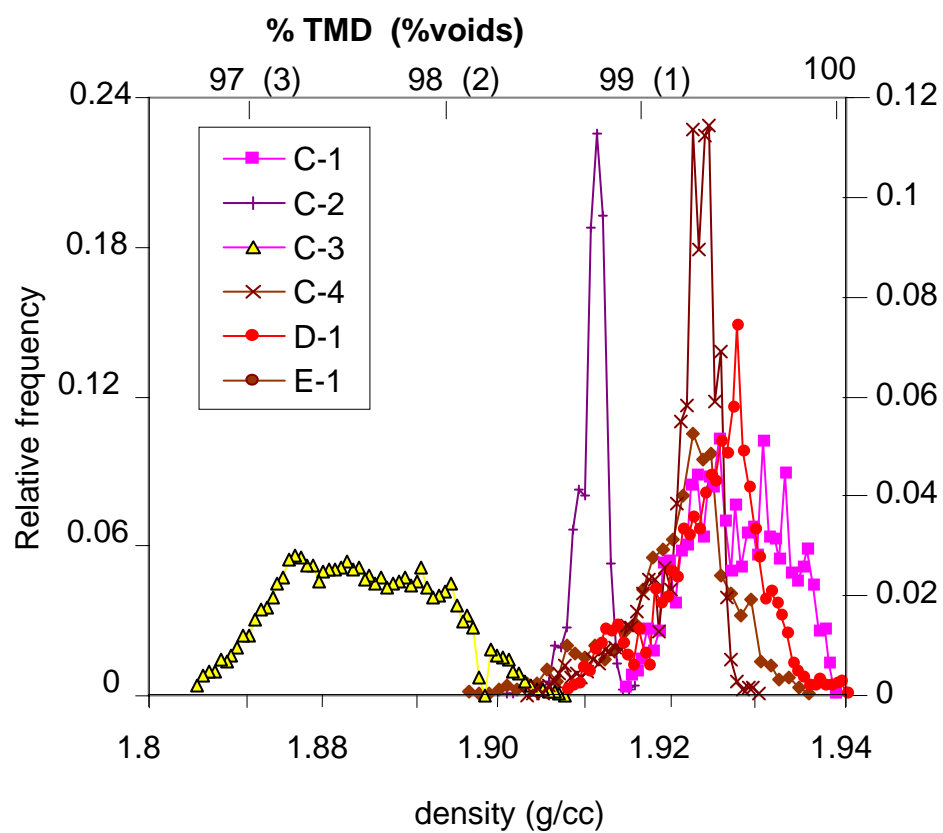


Figure 10. Relative frequencies of the crystal densities of TATB crystallized from EMIMOACh IL/DMSO:20/80.

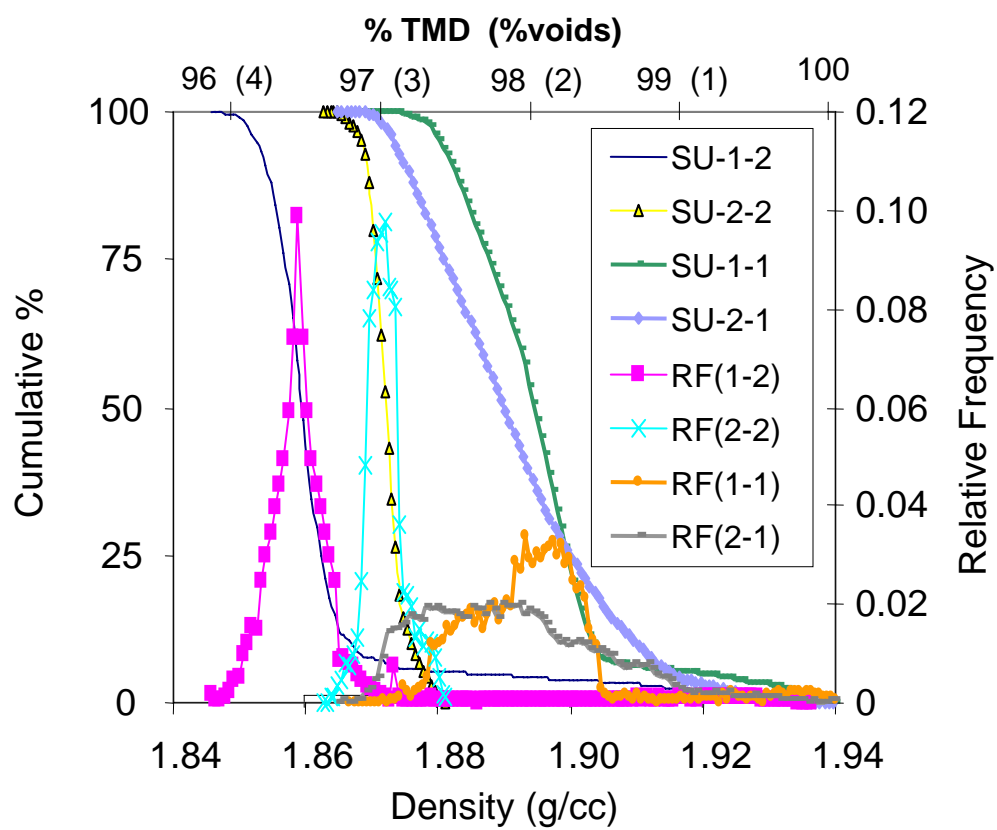


Figure 11. Scale-up EMIMAc/DMSO recrystallization of TATB gave lower density than small scale probably because of long times at 90C°.

1. Sleadd, B., *Synthesis and Scale-up of sym-triaminotrinitrobenzene at Holston Army Ammunition Plant*, in *IM&EM Technology Symposium*. 2006, NDIA: Bristol, UK.
2. Velarde, S., *Pilot Plant Synthesis of Triaminotrinitrobenzene (TATB)*, in *2006 IM/EM Technical Symposium*. 2006, April 24-28, NDIA: Bristol, UK.
3. Hoffman, D.M., et al., *Comparison of New and Legacy TATBs*. Submitted to *Journal of Energetic Materials*, 2007.
4. Armstrong, R.W., Ammon, H. L., Elban, W. L., and Tsai, D. H. , *Investigation of Hot Spot Characteristics in Energetic Crystals*. *Thermochim. Acta*, 2002. **384**: p. 303.
5. Tarver, C.M., Chidester, S. K. and Nichols, A. L. , *Critical Conditions for Impact- and Shock-Induced Hot Spots in Solid Explosives*. *J. Phys. Chem.*, 1996. **100**: p. 5794.
6. Souers, P.C. and P. Vitello, *Initiation pressure thresholds from three sources*. *Propellants Explosives Pyrotechnics*, 2007. **32**(4): p. 288-295.
7. Doherty, R.M. and D.S. Watt, *Relationship Between RDX Properties and Sensitivity*. *Propellants and Explosives*, 2008. **33**(1): p. 4-13.
8. Oxley, J., et al., *A Study of Reduced-Sensitivity RDX*. *Journal of Energetic Materials*, 2007. **25**: p. 141-160.
9. Spyckerelle, C., et al., *Reduced Sensitivity RDX Obtained from Bachmann RDX*. *Propellants, Explosives, Pyrotechnics*, 2008. **33**(1): p. 14-19.
10. Willey, T.M., et al., *Changes in pore size distribution upon thermal cycling of TATB-based explosives measured by ultra-small angle X-ray scattering*. *Propellants Explosives Pyrotechnics*, 2006. **31**(6): p. 466-471.
11. Peterson, P.D. and D.J. Idar, *Microstructural differences between virgin and recycled lots of PBX 9502*. *Propellants Explosives Pyrotechnics*, 2005. **30**(2): p. 88-94.
12. Borne, L., J.-C. Patedoyl, and C. Spycherelle, *Quantitative Characterization of Internal Defects in RDX Crystals*. *Propellants, Explosives, Pyrotechnics*, 1999. **24**: p. 255.
13. van der Heijden, A.E.D.M., et al., *Energetic Materials: Crystallization, Characterization and Insensitive Plastic Bonded Explosives*. *Propellants, Explosives, Pyrotechnics* 2008. **33**(1): p. 25-32.
14. Sharma, J., et al., *The Physical and Chemical Nature of Sensitization Centers Left from Hot Spots Caused in Triaminotrinitrobenzene by Shock or Impact*. *J. Phys. Chem.*, 1987. **91**: p. 5139-5144.
15. Sauer, K.L., et al., *Secondary echoes in three-frequency nuclear quadrupole resonance of spin-1 nuclei*. *J. Chem. Phys.*, 2003. **118**(11): p. 5071-5081.
16. Buess, M.L. and S.M. Caulder, *Factors Affecting the NQR Line Width in Nitramine Explosives*. *Applied Magnetic Resonance*, 2004. **25**: p. 383-393.
17. Erofeev, L.N., Tarasov, Yu. P. , Kalmykov, Yu. B., Shu, Y., Dubikhin, V.V., and Nazin, G.M. , *Crystal defects and stability of RDX*. *Russian Chem. Bull., Int. Ed.* , 2001. **50**(6): p. 1000-1002.
18. Caulder, S.M., et al., *Determining the Crystal Quality of CL-20*, in *JANNAF PDCS CL-20 Technical Exchange Workshop 6-8 May 2003*: Ogden, Utah.

19. Hoffmann, D.M. *Density Distributions in Cyclotrimetylenetrinitramines (RDX)*. in *38th JANNAF Meeting, March 19, 2002*. 2002. Destin, Fl.: Chemical Propulsion Information Agency, Johns Hopkins University, Baltimore, MD.
20. Hoffmann, D.M., *Voids and Density Distributions in 2,4,6,8,10,12-Hexanitro-2,4,6,8,10,12-Hexaazaisowurtzitane (CL-20) Prepared Under Various Conditions*. Propellants, Explosives, Pyrotechnics, 2003. **28**(4): p. 194-200.
21. Borne, L., J. Mory, and F. Schlessler, *Reduced Sensitivity RDX (RS-RDX) in Pressed Formulations: Respective Effects of Intra-Granular Pores, Extra-Granular Pores and Pore Sizes*. Propellants, Explosives, Pyrotechnics, 2008. **33**(1): p. 37-46.
22. Bouma, R.H.B., Hordijk, A. C., van der Steen, A. C., Halvorsen, T. and Skjold, E. *Influence of RDX Crystal Quality and Size on the Sensitivity of RDX Based PBXs*. in *Insensitive Munitions and Energetic Materials Technology Symposium*. 2001. Bordeaux, France.
23. Halvorsen, T., et al., *RS-RDX and RS-HMX: Aging and Shock Sensitivity*, in *36th International ICT- Conference*. 2005: Karlsruhe, Germany.
24. Borne, L., M. Herrmann, and C.B. Skidmore, *Microstructure and Morphology*, in *Energetic Materials Particle Processing and Characterization*, U. Teipel, Editor. 2005, Wiley-VCH. p. 333-366.
25. Low, B.W. and F.M. Richards, *The Use of the Gradient tube for the Determination of Crystal Densities*. J. Am. Chem. Soc.. 1952. **74**(7): p. 1660-1666.
26. Tung, L.H. and W.C. Taylor, *An Improved Method of Preparing Density Gradient Tubes*. J. Polym Sci., 1956. **21**(97): p. 144-147.
27. Foltz, M.F., J.L. Maienschein, and L.G. Green, *Particle size control of 1,3,5-triamino-2,4,6-trinitrobenzene by recrystallization from DMSO*. Journal of Materials Science, 1996. **31**(7): p. 1741-1750.
28. Foltz, M.F., et al., *Recrystallization and solubility of 1,3,5-triamino-2,4,6-trinitrobenzene in dimethyl sulfoxide*. Journal of Materials Science, 1996. **31**(7): p. 1893-1901.
29. Maiti, A., et al., *Fluoride Ionic Liquids: a new class of super-efficient solvents for H-bonded Materials*. Angewende Chemie, 2007(Submitted).
30. Goldstein, J.I., et al., *SEM and X-Ray Microanalysis*. 2 ed. 1992, New York, NY: Plenum Press.
31. Ott, D.G. and T.M. Benziger, *Preparation of 1,3,5-triamino-2,4,6-trinitrobenzene from 3,5 dichloroanisole*. Journal of Energetic Materials, 1987. **5**: p. 343-354.
32. Mitchell, A.R., et al., *A Versatile Synthesis of 1,3,5-Triamino-2,4,6-Trinitrobenzene (TATB)*, in *37th International Institute of Chemical Technology (ICT) Conference*. 2006: Karlsruhe, Germany.
33. Talawar, M.B., et al., *Method for preparation of fine TATB (2-5 μ m) and its evaluation in plastic bonded explosive (PBX) formulations*. Journal of Hazardous Materials, 2006. **137**(3): p. 1848-1852.
34. Han, T.Y., et al., *Solubility and recrystallization of 1,3,5-triamino-2,4,6-trinitrobenzene in 3-ethyl-1-methylimidazolium acetate-DMSO co-solvent system*. Chem. Eur. J., 2008. **in preparation**.

35. Maiti, A., et al., *Solvent screening for a hard-to-dissolve molecular crystal*. Physical Chemistry Chemical Physics, 2008(in preparation).
36. *Stat::Fit*. 2001, Geer Mountain Software: 104 Geer Mountain Road, South Kent, CT 06785.